Phase Behavior of the Melt of Polystyrene−Poly(ethylene oxide) Metallo-Supramolecular Diblock Copolymer with Bulky Counterions

M. Al-Hussein* and W. H. de Jeu

FOM-Institute for Atomic and Molecular Physics, Kruislaan 407, 1098 SJ Amsterdam, The Netherlands

B. G. G. Lohmeijer and U. S. Schubert

Laboratory of Macromolecular Chemistry and Nanoscience and The Dutch Polymer Institute, Eindhoven University of Technology, P O Box 513, 5600 MB Eindhoven, The Netherlands

Received October 28, 2004; Revised Manuscript Received December 29, 2004

ABSTRACT: The melt morphology of polystyrene−poly(ethylene oxide) metallo-supramolecular diblock copolymer has been investigated using small-angle X-ray scattering. The two polymer blocks are linked via a bis(terpyridine)ruthenium(II) ion complex, and tetraphenylborate counterions are used to neutralize the copolymer. A highly ordered lamellar melt with a period of 11.9 nm is obtained by annealing at 55 °C for 40 h. The lamellar structure is composed of segregated domains of the polystyrene and polyethylene blocks with the metal ions and their associated counterions confined to the lamellar interfaces. The lamellar structure disappears during a subsequent heating at 80 °C, leading to a disordered melt. This morphology differs from the spherical aggregates exhibited by the same copolymer melt with smaller hexafluorophosphate counterions, whereby the melt organized into spherical aggregates[1] which underlines the role of the counterions in tuning the final morphology of such supramolecular diblock copolymers.

1. Introduction

Block copolymers self-assemble into well-ordered nanoscale structures[2,3] which makes them of importance in the field of nanotechnology.[4,5] The incorporation of inorganic nanoparticles into block copolymer assemblies adds new physical properties (magnetic, electronic, and optical) as well as reactivity possibilities. Such organic/inorganic composites with nanoscale spatially organized structures are desirable for new electronic and electrooptic devices.[6,7] To this end, many attempts to use block copolymer assemblies as templates for assembling inorganic nanoparticles have been explored. Most of these attempts rely on chemical or physical interactions between one of the blocks and the inorganic nanoparticles.[8,9] Others involve the selective degradation and removal of one microdomain from a microphase-separated polymer film followed by the introduction of inorganic materials into the preformed channels.[10,11] This requires in some cases the synthesis of a special block copolymer. On the other hand, mutually repulsive chemical moieties can also be connected by physical supramolecular interactions (hydrogen bonds, metal ion coordination, or electrostatic interactions) to form block copolymer-like supramolecules.[12−14] In this context, a new strategy to synthesize metallo-supramolecular copolymers, whereby a metal−ligand complex (MLC) is used as a supramolecular linker between the different macromolecules of the copolymer has been developed recently.[15] The self-assembling of such supramolecular copolymers offers a more direct approach for the fabrication of organic/inorganic composites on the nanoscale. In this case, the inorganic nanoparticles are already present in the copolymer chains; thus, steps in the noncohabitation can be saved.

In metallo-supramolecular copolymers, the location and spatial distribution of the inorganic nanoparticles within the polymeric matrix will be determined by the overall morphology of the copolymer. This in turn is the product of the combined effect of the microphase separation of the two polymer blocks and any tendency of the MLCs to self-assemble. To elucidate these factors, we have initiated a research program aiming to understand how the presence of the MLCs affects the ordering of the block copolymers and vice versa. In a previous study, we investigated the melt morphology of one of such metallo-supramolecular diblock copolymers, namely poly(ethylene oxide)−polystyrene metallo-diblock copolymer, PS_{20}−[Ru]−PEO_{70}, by small-angle X-ray scattering.[1] For that copolymer, the bis(terpyridine)ruthenium(II) complex, which has an intrinsic 2+ charge, was used as a supramolecular linker between the PS and PEO blocks. Hexafluorophosphate counterions (PF_6), each with an intrinsic charge 1−, were used to neutralize the block copolymer. The quantitative analysis of the SAXS curves indicated that the MLC ions and their associated counterions tend to form aggregates within the polymer matrix. A liquidlike model of spherical ion−counterion aggregates (radius ∼ 1.5 nm) surrounded by a polymer shell (radius ∼ 2.4 nm) could fit the SAXS curve well. This seemed to be the equilibrium morphology as long annealing in the melt produced essentially no changes in the morphology. In this work, we show that a highly ordered lamellar morphology can be achieved in the melt of the same metallo-diblock copolymer, merely by using the more bulky tetraphenylborate (BPh_4) counterions (see Figure 1a). The lamellar morphology emerges after annealing the copolymer melt for 40 h at 55 °C (above the melting point of the PEO block), which then disappears during a subsequent heating at around 80 °C.

2. Experimental Section

2.1. Samples. The polymer used in this study was synthesized in a multistep process similar to that described in detail elsewhere.[16] In brief, terpyridine-terminated poly(ethylene oxide) (PEO) and polystyrene (PS) precursors were prepared first. This was demonstrated by ^{1}H NMR, ^{13}C NMR, UV/vis,

10.1021/ma047784b CCC: $30.25
Published on Web 03/01/2005

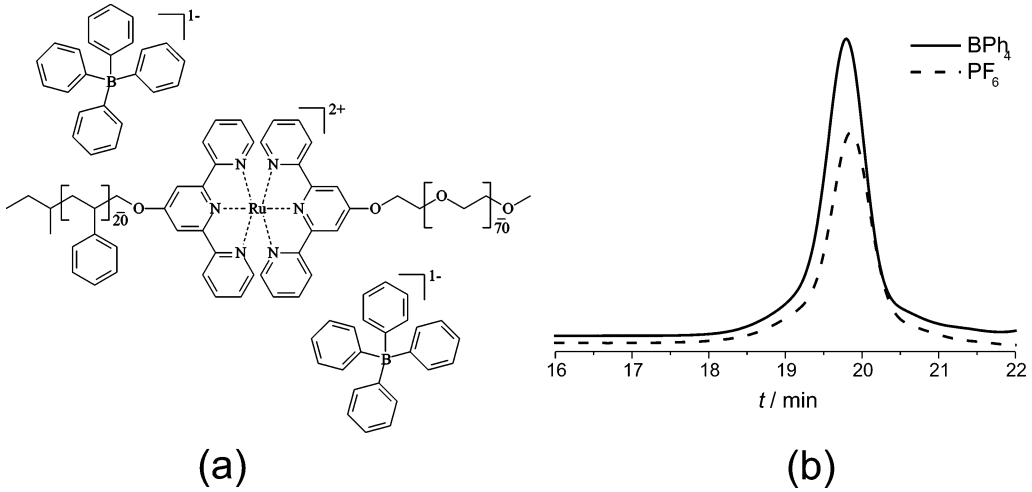

Figure 1. (a) Structure of the PS_{20}−[Ru]−PEO_{70} block copolymer with two tetraphenylborate (BPh_4 counterions. The numbers in the subscript indicate the degree of polymerization. (b) GPC chromatograms of PS_{20}−[Ru]−PEO_{70} with (PF_6) and (BPh_4) counterions.

Table 1. Calculated Volume Fractions of PS, PEO, and the Metal Complex in PS_{20}−[Ru]−PEO_{70} with PDF_6 and BPh_4 Counterions at 55 °C

counterion	V_{PS}/nm^3	V_{PEO}/nm^3	V_{MLC}/nm^3	f_{PS}	f_{PEO}	f_{MLC}
PDF_6	2.00	2.80	0.904	35.1	49.1	15.8
BPh_4	2.00	2.80	1.743	30.6	42.8	26.6

FT-IR, gel permeation chromatography (GPC), and MALDI−TOF MS measurements. The terpyridine-functionalized PEO block was then reacted with $RuCl_3$. The interaction resulted in a PEO monoterpyridine−ruthenium(III) chloride complex, which was isolated and purified. A subsequent reaction of the monocomplex with the terpyridine-functionalized polystyrene under reducing conditions selectively gave rise to an A−B combination, namely an inert heteroleptic (PS−PEO) bis-(terpyridine)ruthenium(II) complex. Figure 1 shows the chemical structure and the GPC chromatograms of PS_{20}−[Ru]−PEO_{70} metallo-supramolecular copolymer with (PF_6) and (BPh_4) counterions. GPC chromatograms of the resulting copolymer looked exactly the same even after prolonged periods of time (typically weeks), indicating that no further exchange took place in the solution. The net charge of the copolymer was neutralized using a counterion exchange. The synthesis inherently gave rise to chloride counterions (coming from the ruthenium(III) chloride mono complex), and those were successfully exchanged by hexafluorophosphate (PF_6) counterions[1] or tetraphenylborate (BPh_4) counterions, as is the case in this study.

2.2. Volume of Metal Ion−Counterion Complex. The density and volume for the bis(terpyridine)ruthenium with and without the two hexafluorophosphate counterions have been reported in the literature.[17] Thus, the volume of the counterions in the complex can be calculated assuming a close packing. However, data on the same complex with tetraphenylborate counterions are not yet available. Therefore, we calculated the volume of the complex with tetraphenylborate counterions using the known volume of the hexafluorophosphate counterions and the ratio of the partial specific volumes of BPh_4 vs PF_6 counterions.[18] For polystyrene and poly(ethylene oxide) the partial volumes can be calculated on the basis of their degrees of polymerization and densities. Hence, the volume fractions of polystyrene, poly(ethylene oxide), and the metal complex can be determined. For amorphous PS and PEO the densities are 1.04 and 1.10 g cm^{-3} at 55 °C, respectively.[19] Table 1 shows the results of the calculations.

2.3. Small-Angle X-ray Scattering. Small-angle X-ray scattering (SAXS) measurements were conducted using an in-house setup with a rotating anode X-ray generator (Rigaku RA-H300) operating at 18 kW. By employing two parabolic multilayer mirrors (Bruker, Karlsruhe), a highly parallel beam of a monochromatic Cu Kα radiation (λ = 0.154 nm) with a divergence of 0.012° was obtained. A Linkam CSS450 shear cell was used as a temperature-controlled sample stage. The SAXS patterns were recorded with a Bruker Hi-Star area detector at a sample-to-detector distance of 1.03 m. The two-dimensional scattering patterns were radially integrated, corrected for the background, and then displayed as one-dimensional plots of the intensity as a function of $q = (4\pi/\lambda)$ sin θ, the modulus of the scattering vector **q**, where 2θ is the scattering angle.

3. Results and Discussion

3.1. Annealed Melt. Figure 2 shows a series of SAXS curves obtained at different times during annealing the copolymer melt at 55 °C. As can be seen, the shape of the curve changes with time. First, it exhibits a single broad peak similar to that reported previously for the (PF_6) counterions,[1] and then after around 10 h at least four new peaks start to develop. The intensities of the new peaks grow with time until they reach their final values after around 40 h. The relative positions of the new peaks (1:2:3:4) indicate a highly ordered lamellar structure of the annealed melt. The first-order peak

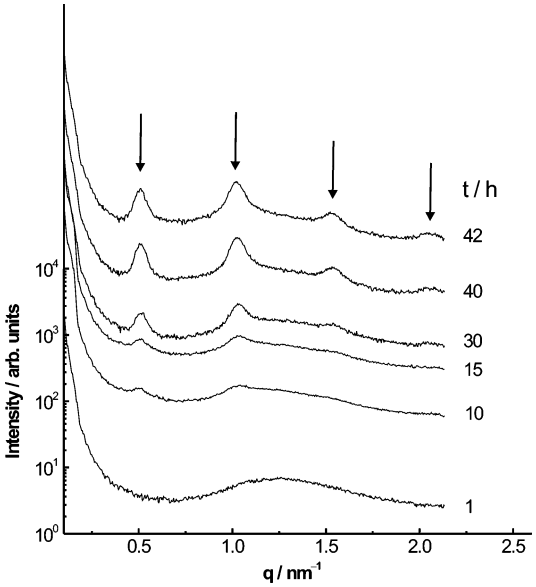

Figure 2. SAXS curves of the PS_{20}−[Ru]−PEO_{70} melt during annealing at 55 °C; arrows indicate the lamellar reflections.

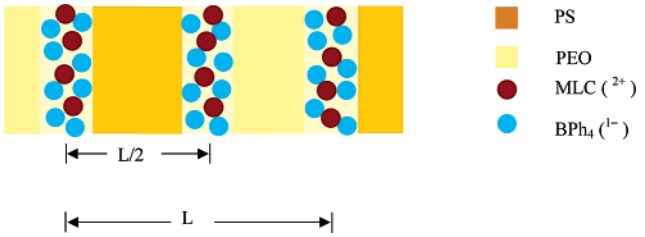

Figure 3. Schematic drawing of possible lamellar structures of the annealed melt of PS_{20}−[Ru]−PEO_{70}. 2+ and 1− indicate the charges on each MC ion and BPh_4 counterion, respectively.

occurs at $q = 0.53$ nm^{-1}, corresponding to a lamellar period of 11.9 nm. We recall here that a conventional PS_{22}-*b*-PEO_{70} diblock copolymer (covalently bonded) with comparable molecular weight and composition showed no microphase separation in the melt.[1] This is not surprising as for such a low molecular weight diblock copolymer microphase separation is inhibited because of the large entropic forces arising from stretching the chains of the two blocks. However, for similar volume fractions but higher molecular weight, microphase separation takes place, and the melt exhibits a lamellar morphology.[19] Hence, it can be concluded the metal ions trigger the microphase separation in the metallo-supramolecular copolymer melt. However, the lamellar morphology and in turn the spatial distribution of the MLCs exhibited by this copolymer is completely different from that with (PF_6) counterions.[1]

3.2. Lamellar Morphology. An interesting feature of the SAXS curve of the annealed melt is the fact that the second-order peak is more intense than the first one. Such a behavior is often seen in the scattering curves of liquid crystalline polymers[20,21] and side-chain liquid crystalline diblock copolymers with a smectic layering.[22] It occurs when the electron densities in the main chain layer and the mesogenic layer are almost equal. In that case, an apparent spacing of half the length of the mesogenic units is induced, making the second order a new fundamental spacing. This offers some clues about the lamellar structure of the annealed copolymer melt. We envisage that the system can effectively be considered as an ABC triblock copolymer, whereby the MLC and its associated counterions act as the middle block (B) that is strongly incompatible with the other two blocks. In that situation, a structure in which the two polymer blocks are microphase separated into lamellae with the MLCs and their counterions confined to the interfaces is obtained (see Figure 3). This entails that the lamellar period L is composed of the sequence A−MLC−BB−MLC−A. The presence of the MLCs and their counterions at the interfaces between the two polymer blocks gives rise to an additional plane of symmetry in the electron density profile. To be more quantitative, we consider Gaussian chains with a radius of gyration $a\sqrt{N/6}$, where a is the statistical segment length and N is the degree of polymerization.[23] Given that $a_{PS} = 0.68$ nm[24] and $a_{PEO} = 0.28$ nm,[25] the corresponding radii of gyration for the PS and PEO chains are 1.24 and 0.96 nm, respectively. Meanwhile, the diameter of a MLC with two BPh_4 counterions is around 1.49 nm, assuming a close-shell packing of the metal complex and the counterions. Consequently, the lamellar period A−MC−BB−MC−A is expected to be $2 \times (2.48 + 1.92 + 1.49) = 11.8$ nm. This is in almost perfect agreement with the experimental value (11.9 nm), indicating that the polymer chains are hardly

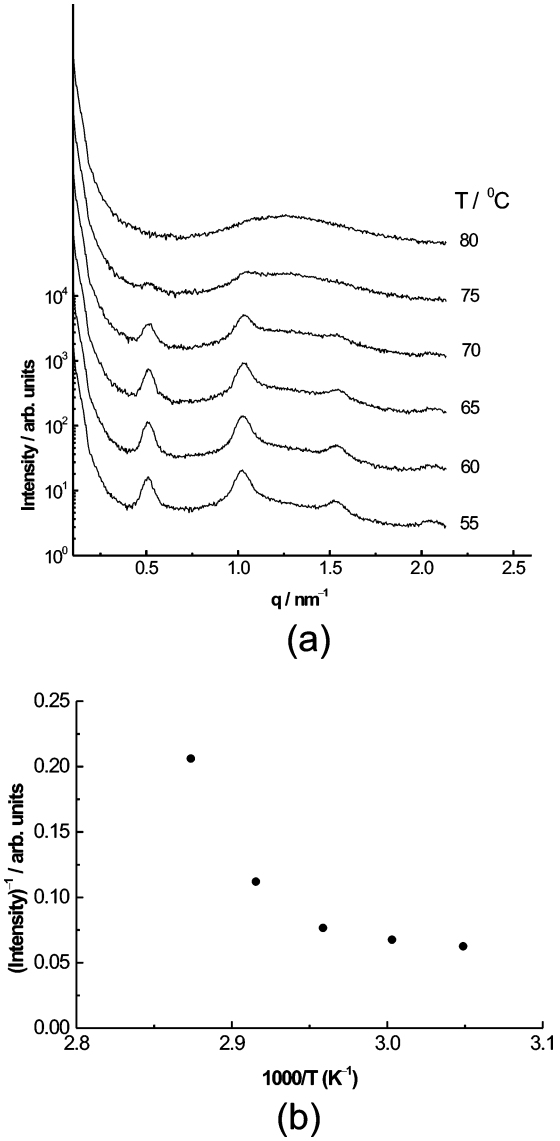

Figure 4. (a) SAXS curves obtained during a subsequent heating of the PS_{20}−[Ru]−PEO_{70} melt after annealing at 55 °C for 42 h. (b) The inverse peak intensity of the first peak against inverse temperature.

stretched. However, the symmetry required to obtain a periodicity of $L/2$ to explain the large second-order intensity is somewhat less perfect: the dimensions of the polymer blocks are around 5 and 4 nm for PS and PEO, respectively. This slight asymmetry is reflected in the angular width of the second-order peak: it is broader than the first one due to the fact that the extra plane of symmetry of the metal ions is not exactly at $L/2$.

Upon cooling the system below 50 °C, crystallization of the PEO block sets in, leading to a new lamellar morphology and a redistribution of the metal ions. More investigations as to how the crystallization conditions affect the new morphology and the packing of the metal ions are underway.

3.3. Disordered Melt. Figure 4a shows a series of SAXS curves during a subsequent heating of the annealed copolymer melt. The peaks disappear at around 80 °C, and instead a single broad peak emerges that is similar to the one exhibited by the copolymer at the early stages of the annealing process. Figure 4b shows the inverse intensity of the first peak against inverse

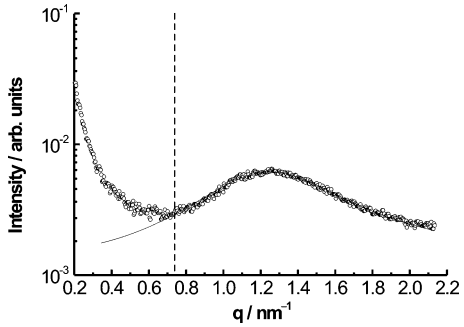

Figure 5. SAXS curve of the PS_{20}−[Ru]−PEO_{70} melt at 80 °C. The solid line is the fit to the Y−C model, and the dashed line indicates the lower limit of the fitting range.

temperature. There is a change in gradient at around 70 °C that defines the ODT, consistent with Leibler's random phase approximation theory.[26] This transition is reversible upon cooling, but more and more time is needed to achieve the lamellar morphology with increasing the annealing temperature. The melt viscosity is expected to decrease with increasing the annealing temperature, and therefore the annealing time should be shorter at high temperatures. On the other hand, the energy barrier for nucleation of the lamellar morphology from the disordered melt is expected to increase with increasing the annealing temperature, and that might explain the longer time needed at high annealing temperatures.

To obtain more quantitative data, we analyzed the corresponding SAXS curves. In both cases the broad peak can be well fitted using the Yarusso−Cooper model[27] of liquidlike modified spheres, which was discussed in more detail elsewhere.[1] Kpl software was used to fit the model to the experimental data.[28] The solid line in Figure 5 represents the resulting fit for the melt curve at 80 °C for q values in the range 0.68−2 nm^{-1}. The best-fit values for the core and the outer shell radii are 0.79 and 2.28 nm, respectively. The core size comes close to the sum of the sizes of a MLC ion and a pair of BPh_4 counterions. This suggests that the MLCs are dispersed uniformly and are not segregated as was the case with (PF_6) counterions. Therefore, we conclude that both the initial melt state and the one above 80 °C are disordered states with the copolymer chains dispersed uniformly in space.

3.4. Influence of Counterions. The results clearly demonstrate the difference between the melt morphology of this copolymer and that studied in our previous study.[1] Since the composition, degree of polymerization, and the metal ion are identical for both copolymers, the change in morphology must be due to differences in the type and size of the two counterions. Our previous study indicates that for small counterions the metal ions and their associated counterions have a strong tendency to associate into spherical aggregates, causing the two polymer blocks to intermix. Evidently, replacing the counterions with more bulky ones leads to a dramatic change in the final morphology. This can be used to tune the morphology of the metallo-supramolecular copolymers with a minimum number of steps. In a different context Heeger et al.[29] studied the role of functionalized counterions in conjugated polyelectrolyte−surfactant complexes. They showed that, by a judicious choice of a functional group attached to the counterion, a high molecular weight conducting polymer can be made soluble in a variety of common organic solvents and be compatible with thermoplastic polymers that have similar molecular structure. Levon et al.[30] investigated the effect of such functionalized counterions on self-assembly. They reported a smectic-like layered structure, whereby the hydrophobic tails of the counterions act as spacers between parallel stacks of the main chains. The same concept has also been used in coordinated self-assembled materials. Kurth et al.[31] used oligomeric construction units while Ikkala et al.[32] polymeric construction units and the self-assembled structures could be tuned by the amphiphilic counterions. In all these examples, the counterions were surfactant-like, whereby the long aliphatic tail of the amphiphile counterion plays a major role in providing the driving force for the self-assembling process, which is not the case in our system.

Changing the size and/or the interaction energies of the counterions with the polymer blocks is expected to lead to changes in the self-assembly of the MLC ions and their counterions. Employing the ABC triblock copolymer analogue, three additional parameters will contribute to the total free energy of the system comparing to a diblock copolymer. The first parameter is the volume fraction of the metal ion−counterion complex, while the other two are the effective interaction parameters between the metal ion−counterion complex and the PS and PEO blocks. This, in turn, leads to differences in the equilibrium morphology and the phase behavior of the metallo-supramolecular copolymer. The results presented thus far are in a qualitative agreement with theoretical predictions on the microphase separation transition in ABC block copolymers with a strongly interacting B block reported by Stadler and coworkers.[33] It was found that the size and interactions of the middle block affect the miscibility of the outer blocks (A and C). A long middle block can enhance the miscibility of the outer blocks, whereas a short strongly interacting middle block has an opposite effect leading to a continuous microphase separation at $T_{ODT}^{ABC} = {}^5/_3\, T_{ODT}^{AC}$. Floudas et al. were the first to corroborate these theoretical predictions experimentally.[34] They have shown that, by inserting a short ionic group (zwitterion) at the junction of diblock copolymers of polystyrene and polyisoperene (PS-*b*-PI), another level of microphase separation between the ionic and the hydrocarbon materials, on top of the segregation between the two hydrocarbon blocks, is formed. They have also shown that the presence of the zwitterionic group decreases the miscibility of the PS−PI diblock, raising T_{ODT} 5 °C above that of the diblock. In our case, however, there is no T_{ODT} for the PS-*b*-PEO diblock copolymer, and it is the metal ions and their associated counterions which induce the microphase separation in the PS_{20}−[Ru]−PEO_{70} copolymer.

4. Conclusions

We have shown that a highly ordered lamellar structure develops in the melt of a metallo-supramolecular PS_{20}−[Ru]−PEO_{70} diblock copolymer when bulky counterions are used. Considering the system as a triblock copolymer, whereby the MLC and its associated counterions act as a middle block that is strongly incompatible with the other two blocks, gives rise to such a lamellar structure in which the two polymer blocks are microphase separated into lamellae with the MLCs and their counterions confined to the interfaces. The results indicate an important role for the type and

the size of the counterions in determining the final morphology of metallo-supramolecular diblock copolymers.

Acknowledgment. This work is part of the research program of the "Stichting voor Fundamenteel Onderzoek der Materie (FOM)", which is financially supported by the "Nederlandse Organisatie voor Wetenschappelijk Onderzoek (NWO)". M.A.H. thanks Dr. W. Stille (Universität Freiburg) for providing the Kpl software and gratefully acknowledges financial support by the EU-network POLYNANO under Contract HPRN-CT-1999-00151. B.G.G.L. and U.S.S. thank NWO, the Dutch Polymer Institute (DPI), and the Fonds der Chemischen Industrie for funding.

References and Notes

(1) Al-Hussein, M.; Lohmeijer, B. G. G.; Schubert, U. S.; de Jeu, W. H. *Macromolecules* **2003**, *36*, 9281.
(2) Bates, F. M.; Fredrickson, G. H. *Annu. Rev. Phys. Chem.* **1990**, *41*, 525.
(3) Hamley, I. W. *The Physics of Block Copolymers*; Oxford: New York, 1998.
(4) Park, M.; Harrison, C. K.; Chaikin, P. M.; Register, R. A.; Adamson, D. H. *Science* **1997**, *276*, 1407.
(5) Park, C.; Yoon, J.; Thomas, E. L. *Polymer* **2003**, *44*, 6725.
(6) Fink, Y.; Urbas, A. M.; Bawendi, M. G.; Joannopoulos, J. D.; Thomas, E. L. *J. Lightwave Technol.* **1999**, *17*, 1963.
(7) Jeoung, E.; Galow, T. H.; Schotter, J.; Bal, M.; Ursache, A.; Tuominen, M. T.; Stafford, C. M.; Russell, T. P.; Rotello, V. M. *Langmuir* **2001**, *17*, 6396.
(8) Bockstaller, M. R.; Kolb, R.; Thomas, E. L. *Adv. Mater.* **2001**, *13*, 1783.
(9) Lopes, W. A. *Phys. Rev. E* **2002**, *65*, 031606.
(10) Thurn-Albrecht, T.; Schotter, J.; Kästle, G. A.; Emley, N.; Shibauchi, T.; Krusin-Elbaum, L.; Guarini, K.; Black, C. T.; Tuominen, M.; Russell, T. P. *Science* **2000**, *290*, 2126.
(11) Kim, H.; Jia, X.; Stafford, M.; Kim, D.; McCarthy, T. J.; Tuominen, M.; Hawker, C. J.; Russell, T. P. *Adv. Mater.* **2001**, *13*, 795.
(12) Sijbesma, R. P.; Meijer, E. W. *Chem. Commun.* **2003**,, 5.
(13) Ikkala, O.; ten Brinke, G. *Science* **2002**, *295*, 2407.
(14) Antonietti, M. *Nat. Mater.* **2003**, *2*, 9.
(15) (a) Schubert, U. S.; Eschbaumer, C. *Macromol. Symp.* **2001**, *163*, 177. (b) Schubert, U. S.; Eschbaumer, C. *Angew. Chem.* **2002**, *41*, 2892.
(16) Lohmeijer, B. G. G.; Schubert, U. S. *Angew. Chem., Int. Ed.* **2002**, *41*, 3825.
(17) Pyo, S.; Pérez-Cordero, E.; Bott, S. G.; Echegoyen, L. *Inorg. Chem.* **1999**, *38*, 3337.
(18) Marcus, Y.; Hefter, G. *Chem. Rev.* **2004**, *104*, 3405.
(19) Zhu, L.; Cheng, S. Z. D.; Calhoun, B. H.; Ge, Q.; Quirk, R. P.; Thomas, E. L.; Hsiao, B. S.; Yeh, F.; Lotz, B. *Polymer* **2001**, *42*, 5829.
(20) Shibaev, V. P., Lam, L., Eds. *Liquid Crystalline and Mesomorphic Polymers*; Springer-Verlag: New York, 1994.
(21) Nieuwhof, R. P.; Marcelis, A. T. M.; Sudhölter, E. J. R.; Picken, S. J.; de Jeu, W. H. *Macromolecules* **1999**, *32*, 1398.
(22) Al-Hussein, M.; de Jeu, W. H.; Vranichar, L.; Pispas, S.; Hadjichristidis, N.; Itoh, T.; Watanabe, J. *Macromolecules* **2004**, *37*, 6401.
(23) Strobl, G. *The Physics of Polymers*; Springer: Berlin 1996.
(24) Helfand, E.; Wasserman, Z. R. *Macromolecules* **1980**, *13*, 994.
(25) Reiter, G.; Vidal, L. *Eur. Phys. J. E* **2003**, *12*, 497.
(26) Leibler, L. *Macromolecules* **1980**, *13*, 1602.
(27) Yarusso, D. J.; Cooper, S. L. *Macromolecules* **1983**, *16*, 1871.
(28) Stille, W. http://frsl06.physik.uni-freiburg.de/privat/stille/kpl/, 2003.
(29) Cao, Y.; Smith, P.; Heeger, J. *Synth. Met.* **1992**, *48*, 91.
(30) Zheng, W.-Y.; Wang, R.-H.; Leveon, K.; Rong, Z. Y.; Taka, T.; Pan, W. *Macromol. Chem. Phys.* **1995**, *196*, 2443.
(31) Kurth, D. G.; Lehmann, P.; Schuette, M. *Proc. Natl. Acad. Sci. U.S.A.* **2000**, *97*, 5704.
(32) Valkama, S.; Lehtonen, O.; Lappalainen, K.; Kosonen, H.; Castro, P.; Repo, T.; Torkkelo, M.; Serimaa, R.; ten Brinke, G.; Leskela, M.; Ikkala, O. *Macromol. Rapid Commun.* **2003**, *24*, 556.
(33) Erukhimovich, I.; Volker, A.; Stadler, R. *Macromolecules* **1997**, *30*, 7435.
(34) Pispas, S.; Floudas, G.; Hadjichristidis, N. *Macromolecules* **1999**, *32*, 9074.

MA047784B